Applied Clay Science 120 (2016) 9–15

Contents lists available at ScienceDirect

Applied Clay Science

journal homepage: www.elsevier.com/locate/clay

# Efficiency of Fe–montmorillonite on the removal of Rhodamine B and hexavalent chromium from aqueous solution

Lingya Ma [a,b,c], Yunfei Xi [a,*], Hongping He [b,d,**], Godwin A. Ayoko [a], Runliang Zhu [b,d], Jianxi Zhu [b,d]

[a] Nanotechnology and Molecular Science Discipline, Faculty of Science and Engineering, Queensland University of Technology (QUT), 2 George Street, GPO Box 2434, Brisbane, QLD 4000, Australia
[b] Key Laboratory of Mineralogy and Metallogeny, Guangzhou Institute of Geochemistry, Chinese Academy of Sciences, Guangzhou 510640, China
[c] University of Chinese Academy of Sciences, Beijing 100049, China
[d] Guangdong Provincial Key Laboratory of Mineral Physics and Material, Guangzhou 510640, China

ARTICLE INFO

*Article history:*
Received 30 September 2015
Received in revised form 6 November 2015
Accepted 7 November 2015
Available online xxxx

*Keywords:*
Simultaneous adsorption
Fe–montmorillonite
Hexavalent chromium
Rhodamine B

ABSTRACT

Fe–montmorillonite (Fe–Mt) was prepared and tested for its potential application in the simultaneous removal of hexavalent chromium (Cr(VI)) and rhodamine B (RhB) from aqueous solution. The adsorption kinetics and capacities of Fe–Mt toward Cr(VI) and RhB were determined in relation to the initial contaminant concentration, pH of the solution and concentration of coexist contaminant. The adsorption kinetics of Cr(VI) or/and RhB in both single and simultaneous systems were investigated, which showed that an equilibrium time of a few hours was needed for the adsorption of Cr(VI) and RhB on Fe–Mt. The pseudo-second order model offers a better fit than pseudo-first order model for the Cr(VI) and RhB adsorption. Compared with the single adsorption systems, adsorption rates and quantities of Cr(VI) and RhB adsorbed on Fe–Mt were slightly enhanced in the simultaneous adsorption system. The most effective pH range for the removal of Cr(VI) and RhB was found to be 3.0–4.0. Cr(VI) adsorption isotherms were best represented by the two-site Langmuir model while RhB isotherms followed the Freundlich model. For both contaminants, the adsorption of one contaminant increases with increase in the initial concentration of the other one. Therefore, Fe–Mt could simultaneously remove Cr (VI) and RhB from water. The properties of Fe–Mt were characterized by X-ray diffraction (XRD), scanning electron microscope (SEM), and thermogravimetric analysis (TG). The findings of this study provide novel information for the development of clay-based adsorbents toward dyes and heavy metals.



## 1. Introduction

One of the negative effects of over industrialization is that various toxic chemicals are released from industry sites into water and soil. For example, wastewaters from leather tanning, textile, paper and many other industries always contain considerable amount of dyes and heavy metals. Rhodamine B (RhB) and hexavalent chromium (Cr (VI)) are widely used in such industries. Being carcinogen chemicals, Cr(VI) and RhB are not only harmful to the environment but also becoming a potential threat to the health of animals and human beings (Fisher, 1999; Sparks, 2005; USEPA, 2014). Hence, removal of both contaminants from wastewater has a high priority. Adsorption is generally considered as one of the most economical and effective methods for the removal of these contaminants from water and various adsorbents have been developed (Yuan et al., 2009; Yuan et al., 2010; Ding et al., 2014; Salgado-Gómez et al., 2014). However, few studies were focused on simultaneous adsorption of both contaminants, since they often coexist in the wastewater and their fate and transport may be significantly affected by each other.

Montmorillonite is an example of naturally abundant clay minerals that have been widely used in environmental remediation (Bergaya and Lagaly, 2013). Unmodified montmorillonite can efficiently remove cationic contaminants (e.g. RhB) from water through cation exchange of its original cations in the interlayer space (Undabeytia et al., 1998; Selvam et al., 2008; Yuan et al., 2013; Bhattacharyya et al., 2014). However, because of the permanent negative charged layer surface, it has a poor affinity for anionic contaminants (e.g. oxyanion of Cr(VI)) (Zhou et al., 2010). Interestingly, poly-hydroxyl metal modified montmorillonite (Hy–Mt) exhibit a strong affinity for both cationic and anionic contaminants due to the high reactivity of the surface hydroxyl groups (Karamanis and Assimakopoulos, 2007; Schlegel and Manceau, 2007; Yan et al., 2008; Wu et al., 2009; Yan et al., 2010; Zhu et al., 2014; Ma et al., 2015). As a low-cost adsorbent, the adsorption behaviours of poly-hydroxyl iron modified montmorillonite (Fe–Mt) toward ionic dyes or oxyanions from water have received a lot of attention (Borgnino et al., 2010; Zhou et al., 2010; Hou et al., 2011). Previous studies showed that Fe–Mt has very good adsorption capacities toward RhB

* Corresponding author.
** Correspondence to: H. He, Key Laboratory of Mineralogy and Metallogeny, Guangzhou Institute of Geochemistry, Chinese Academy of Sciences, Guangzhou 510640, China.
*E-mail addresses:* y.xi@qut.edu.au (Y. Xi), hehp@gig.ac.cn (H. He).

http://dx.doi.org/10.1016/j.clay.2015.11.010
0169-1317/

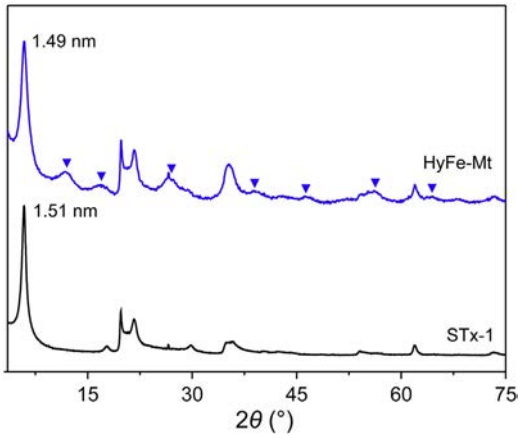


**Fig. 1.** X-ray diffraction (XRD) patterns of Mt and Fe–Mt. The reflections labelled ▼ belong to polyhydroxy-iron (primary akaganeite).

or Cr(VI) (Zhou et al., 2010; Hou et al., 2011). However, the simultaneous adsorption behaviours of these contaminants on Fe–Mt were seldom mentioned.

The adsorption mechanism of oxyanions on Hy–Mt might be ligand exchange, i.e. the replacement of surface hydroxyls by oxyanions, and then the adsorbed oxyanion may form inner-sphere complexes on the surface of Hy–Mt (Zhu and Zhu, 2007; Zhu et al., 2014; Ma et al., 2015). For the cationic contaminants, they can be adsorbed on Hy–Mt through cation exchange, and the exchangeable cation may originate from interlayer metal cations and/or the proton from the surface hydroxyl groups (Matthes et al., 1999; Zhu et al., 2014). As oxyanions and cationic contaminants might have same adsorption sites on the surface of Fe–Mt, the simultaneous adsorption behaviours of Cr(VI) and RhB on Fe–Mt are worth studying.

In this study, the simultaneous adsorption behaviours of Cr(VI) and RhB on the surface of Fe–Mt were investigated. Fe–Mt was prepared from a combination of polymeric hydroxyiron and montmorillonite and characterized by X-ray diffraction (XRD), scanning electron microscope (SEM), and thermogravimetric analysis (TG). Adsorptions in single and simultaneous systems were studied and the effects of pH and initial concentration of coexist contaminant were evaluated. Adsorption kinetics and equilibrium isotherms were also investigated to reveal the adsorption rates, maximum capacities and possible mechanism of Cr (VI) and RhB adsorption on Fe–Mt.

## 2. Materials and methods

### 2.1. Materials

The Ca-montmorillonite (STx-1) was purchased from the Source Clay Mineral Repository (Columbia, MO, USA) and was denoted as Mt. The cation exchange capacity (CEC) is 84.4 meq/100 g. The Rhodamine B (RhB), with purity >95%, was purchased from Sigma-Aldrich. The $K_2Cr_2O_7$, $Na_2CO_3$ and $FeCl_3$ were supplied by Chem-Supply Pty. Ltd., Australia. All chemicals were analytical grades and used without further purification.

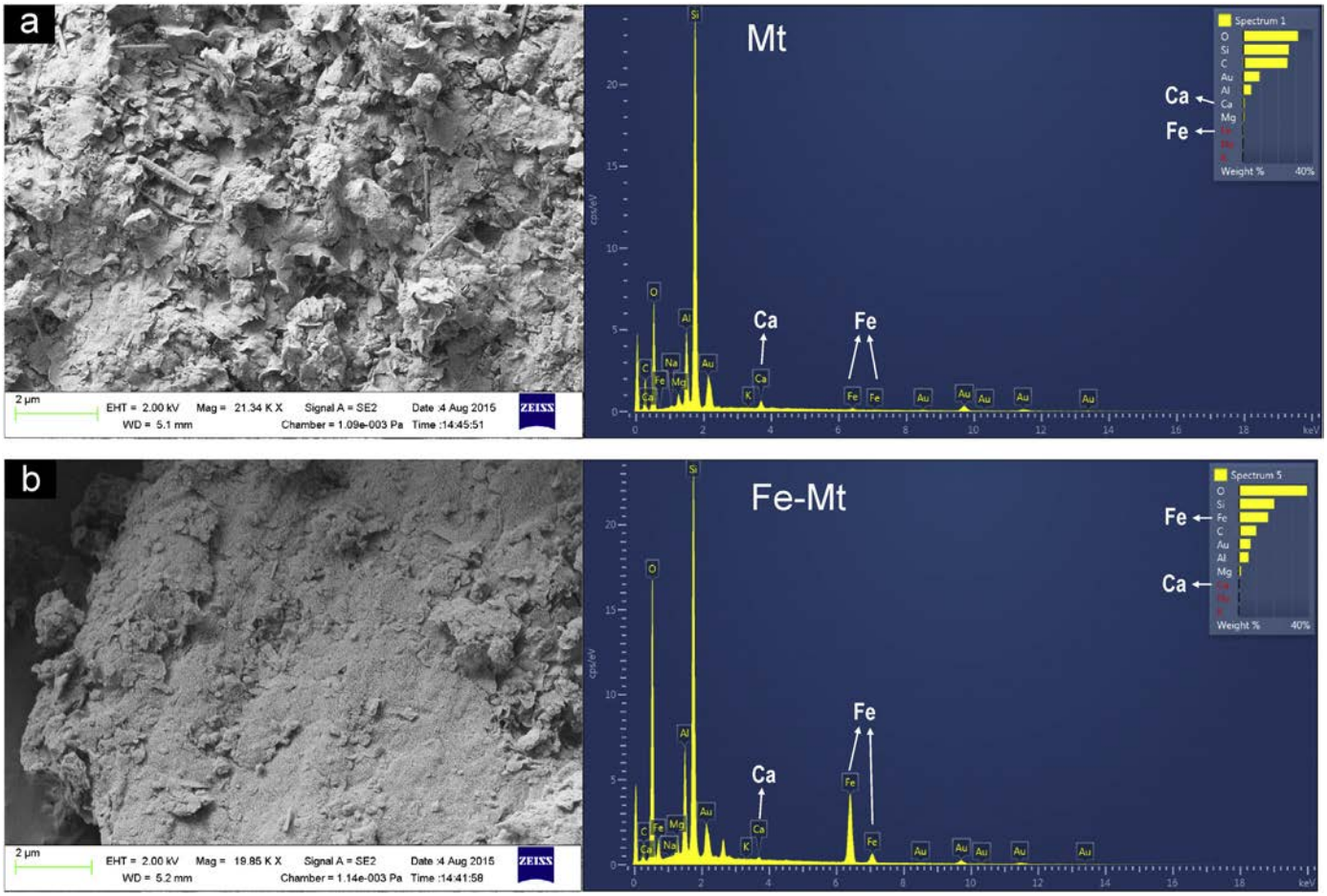


**Fig. 2.** EDX and SEM images of (a) Mt and (b) Fe–Mt.

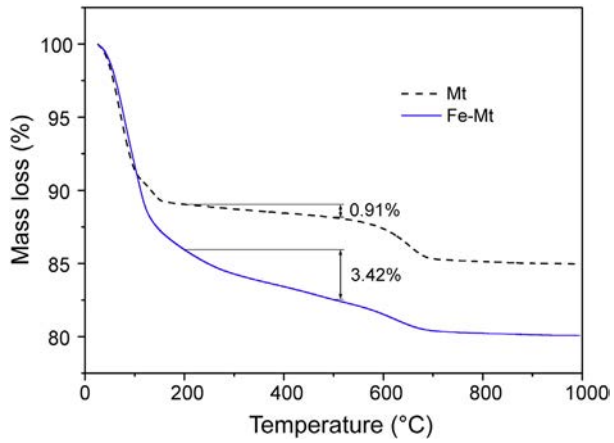


**Fig. 3.** TG curves of raw Mt and Fe–Mt.

### 2.2. Preparation of Fe–montmorillonite

Preparation of Fe–Mt was undertaken by a similar procedure described previously (Yuan et al., 2008; Wu et al., 2009).The solution containing poly-hydroxyl iron was prepared as follows: 1 M $Na_2CO_3$ solution was prepared and added dropwise into a 0.25 M $FeCl_3$ solution under vigorous stirring. The final OH/Fe molar ratio was 2.0. Under continuous stirring for 12 h, the resultant solution was aged for another 12 h at room temperature for further use.

5 g of Mt was dispersed into 100 ml of deionized water. The poly-hydroxyl iron solution was added slowly into the clay mineral dispersion which was kept under vigorous stirring in a water bath at 60 °C until a ratio of 10 mmol Fe per gramme of clay mineral was reached; after addition of the pillaring solution, the reaction mixture was stirred for 12 h, and then aged for 12 h at 60 °C. The mixture was filtered and washed with distilled water until chloride ions were completely removed. The product was air-dried at 50 °C overnight and denoted as Fe–Mt.

### 2.3. Characterization of adsorbents

Powder X-ray diffraction (XRD) patterns were collected using Ni-filtered CuKα radiation (λ = 0.154 nm on a PANalytical X'Pert PRO MPD diffractometer which was operated at 40 kV and 40 mA with 0.5° divergence slit and 1.52 mm anti-scatter slit between 3.5° and 75° (2θ) at a step size of 0.0167°.

Thermogravimetric analysis (TG) was performed on a TGA-Q500, TA Instruments Inc. USA. The samples were heated from room temperature to 1000 °C at a rate of 10 °C/min under a flow of high-purify nitrogen (40 ml/min).

A Zeiss Sigma field scanning electron microscope (FESEM) with integrated energy dispersive X-ray analyser (EDX) system was used for morphological studies. All samples were coated with gold before the SEM studies.

### 2.4. Adsorption experiments

The uptakes of Cr(VI) and RhB were investigated via equilibration and kinetic measurements at pH 4. For the equilibration measurement, both Cr(VI) and RhB were adsorbed simultaneously on Fe–Mt. The initial concentration of one contaminant was 5–50 mg/L for Cr(VI) or 80–320 mg/L for RhB, the other one was kept as a constant at 200 mg/L for RhB or 15 mg/L for Cr(VI). In the case of kinetic measurement, the adsorptions of Cr(VI) and RhB in both single and binary systems were investigated with the initial concentration of 15 mg/L for Cr (VI) or/and 200 mg/L for RhB.

Batch experiments were performed at room temperature using glass reactors under stirring to investigate the adsorption capacity of Fe–Mt (1 g/L) in aqueous solution. The adsorbent was separated by centrifugation at 5000 rpm for 5 min. The initial pHs of the dispersions were adjusted using 0.1 M HCl and NaOH. The concentration of Cr(VI) in the supernatant was determined by inductively coupled plasma optical emission spectrometer (ICP-OES, Perkin Elmer Optima 8300 DV) and that of RhB was analysed on a UV–Vis spectrophotometer (Agilent Technologies Cary 60) at a wavelength of 553 nm. Control experiments indicated no loss of both contaminants in solution in the adsorption process with no interference occurred between two contaminants during their analysis.

### 2.5. Desorption experiments

Desorption studies were conducted by removing the supernatant after the adsorption equilibrium, replacing the solution with an equal volume of 0.01 M KCl solution at pH 4, and then shaking for 24 h. These steps were repeated three times and the concentrations of Cr (VI) and RhB in the supernatant after each desorption cycle were determined. The initial concentrations of adsorption were 15 mg/L for Cr(VI) and 200 mg/L for RhB.

## 3. Results and discussion

### 3.1. Characterization of adsorbent

The structures of the raw Mt and Fe–Mt were investigated using XRD, SEM and TG. The $d_{001}$-values of Mt and Fe–Mt were comparable,

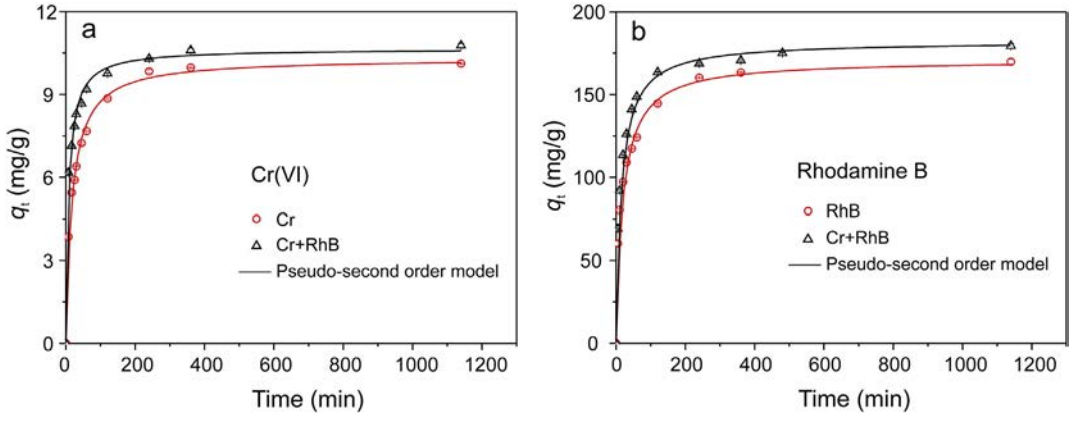


**Fig. 4.** Adsorption kinetics of Cr(VI) (a) and RhB (b) on Fe–Mt (1 g/L) in single (Cr or RhB) and simultaneous (Cr + RhB) systems.($C_{0,\,Cr}$ = 15 mg/L, $C_{0,\,RhB}$ = 200 mg/L).

1.51 nm for Mt and 1.49 nm for Fe–Mt (Fig. 1). According to Yuan et al. (2008), compared with raw Ca-montmorillonite (Ca–Mt), the d-value of Fe-pillared Ca–Mt slightly decreased to 1.47 nm (similar value obtained in this study) due to the cation exchange of the original $Ca^{2+}$ by hydroxyiron cations. The appearance of several weak reflections at ~11.8, 16.8, 26.7, 39.2, 46.4, and 55.9° 2θ in the pattern of Fe–Mt is consistent with the formation of polymeric hydroxyiron species, suggesting the successful loading of hydroxyiron on montmorillonite (Zhu et al., 2014).

According to the EDX and SEM images of Mt and Fe–Mt, Mt had a face-to-edge structure between particles with random orientation (Fig. 2a). With the loading of hydroxyiron, Fe–Mt had relatively smaller particles and some smaller pores on the surface (Fig. 2b). Elemental composition of the surface was determined by EDX. Compared with Mt, iron content on the surface of Fe–Mt sharply increased after hydroxyiron loading but calcium content dramatically decreased to trace (Fig. 2b), indicating the calcium irons were exchanged by hydroxyirons. More loaded hydroxyiron could provide more reactive adsorption sites for the contaminants (Zhu and Zhu, 2007; Zhu et al., 2009). However for the content of calcium,

The TG analyses for the samples were also studied (Fig. 3). In the curve of Mt, two major mass losses were observed: the mass loss below 200 °C was due to the removal of physical-adsorbed water while that at 500–700 °C was ascribed to the dehydroxylation of the layer structure. Similar to that in Mt, the TG curve of Fe–Mt showed a large mass loss below 200 °C from the evaporation of adsorbed water, and a mass loss in the range of 200–700 °C due to the dehydroxylation of hydroxyiron and the layer structure (Yuan et al., 2008). In the temperature range of 200–500 °C, the mass loss of Fe–Mt mainly corresponded to the dehydroxylation of loaded hydroxyiron since the absence of evident mass loss on the TG curve of Mt. The larger mass loss of Fe–Mt (3.42%) than that of STx-1 (0.91%) in this range suggested the existence of hydroxyiron on Fe–Mt, which was consistent with the EDX results.

According to the above characterization, the hydroxyiron successfully loaded on Mt, but the iron aggregates mainly loaded on the external surface of Mt and interparticle pores (Yuan et al., 2008), and the intercalated ions might be hydroxyiron ions with small size.

### 3.2. Adsorption kinetics

The adsorption kinetics of Cr(VI) and RhB on Fe–Mt in both single and simultaneous systems were investigated. In both systems, Fe–Mt displayed quite high removal percentages toward Cr(VI) (69–71%) and RhB (85–91%) (Fig. 4). All adsorption processes were very fast at the beginning, and then progressed and plateaued within 360 min (Fig. 4). Compared with adsorptions in the single system, more of the two contaminants were adsorbed in the simultaneous system, indicating that Cr(VI) and RhB were adsorbed synergistically in the latter system.

In order to better understand the adsorption behaviours of Cr(VI) and RhB on Fe–Mt, both Lagergen's pseudo-first order equation (Eq. (1)) and pseudo-second order equation (Eq. 2) were used to analyse the adsorption of Cr(VI) and RhB on Fe–Mt (Ho and McKay, 1999; Karamanis and Assimakopoulos, 2007).

**Table 1**
Kinetic parameters for Cr(VI) and Phodamine B (RhB) adsorption onto Fe–Mt.

| Adsorbates | Pseudo-first-order model | | | Pseudo-second-order model | | |
|---|---|---|---|---|---|---|
| | $q_e$ (mg/g) | $k_1$ (1/min) | $R^2$ | $q_e$ (mg/g) | $k_2$ (g/mg·min) | $R^2$ |
| Single system | | | | | | |
| Cr(VI) | 9.53 | 0.0382 | 0.9539 | 10.31 | $5.40 \times 10^{-3}$ | 0.9939 |
| RhB | 157.23 | 0.0357 | 0.9638 | 170.89 | $2.97 \times 10^{-4}$ | 0.9948 |
| Simultaneous system | | | | | | |
| Cr(VI) | 10.04 | 0.0722 | 0.9560 | 10.65 | $1.14 \times 10^{-2}$ | 0.9952 |
| RhB | 170.52 | 0.0422 | 0.9863 | 182.12 | $3.55 \times 10^{-4}$ | 0.9920 |

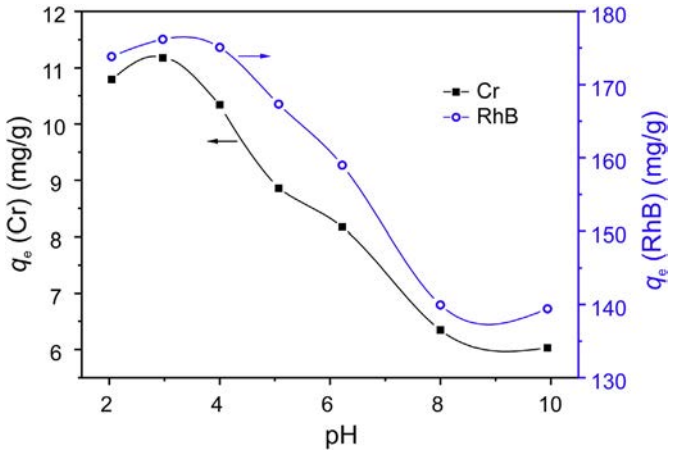


**Fig. 5.** Effect of pH on simultaneous adsorption of Cr(VI) ($C_{0,\ Cr} = 15$ mg/L) and RhB ($C_{0,\ RhB} = 200$ mg/L) on Fe–Mt (1 g/L).

$$\frac{dq_t}{dt} = k_1 \cdot (q_e - q_t) \tag{1}$$

$$\frac{dq_t}{dt} = k_2 \cdot (q_e - q_t)^2. \tag{2}$$

Integrating Eqs. (1) and (2) for the boundary condition $q_t = 0$ to $q_t = q_t$ at $t = 0$ to $t = t$, the equations can be given as:

$$q_t = q_e\left(1 - e^{-k_1 t}\right) \tag{3}$$

$$\frac{t}{q_t} = \frac{1}{k_2 q_e^2} + \frac{1}{q_e} t. \tag{4}$$

where $q_e$ (mg/g) and $q_t$ (mg/g) are the amount of solute adsorbed by adsorbent at equilibrium and at time t (min), respectively; $k_1$ (1/min) and $k_2$ (g/mg·min) are the rate constants of pseudo-first and pseudo-second order models, respectively. Compared with the linear correlation coefficient $R^2$, kinetic data for the adsorption of both Cr(VI) and RhB on Fe–Mt in two systems were in good agreement with the pseudo-second order rate equation (Table 1). Besides $q_e$ values, $k_2$ values of Cr(VI) and RhB adsorption in the simultaneous system were slightly larger than that in the single systems (Table 1), indicating that Fe–Mt could simultaneously remove both contaminants at faster rates than that in the single systems, especially for the adsorption of Cr(VI).

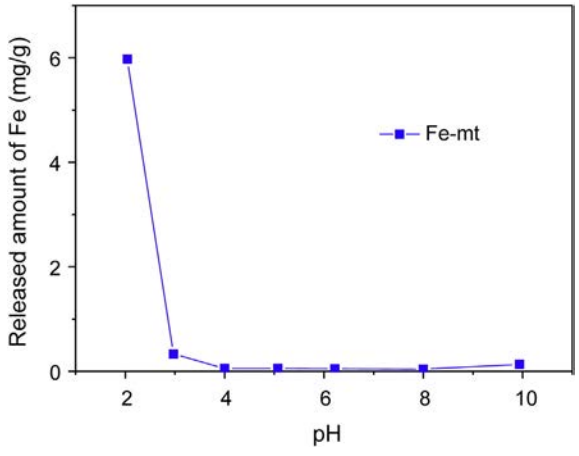


**Fig. 6.** The released amount of Fe ions from Fe–Mt at various pHs.

**Table 2**
Langmuir and Freundlich equation parameters for the simultaneous adsorption of Cr(VI) and Rhodamine B (RhB) onto hydroxyiron-montmorillonite.

| Values and parameters | Cr(VI) | RhB |
|---|---|---|
| Freundlich | | |
| $K_F$ | 8.70 ± 0.26 | 115.89 ± 2.54 |
| $1/n$ | 0.12 ± 0.01 | 0.156 ± 0.006 |
| $R^2$ | 0.970 | 0.994 |
| SD(%) | 5.80 | 2.01 |
| One-site Langmuir | | |
| $Q$ (mg/g) | 11.75 ± 0.59 | 205.73 ± 16.53 |
| $K$ (L/mg) | 25.91 ± 13.29 | 1.56 ± 1.03 |
| $R^2$ | 0.761 | 0.665 |
| SD(%) | 13.14 | 28.73 |
| Two-site Langmuir | | |
| $Q_1$ (mg/g) | 7.74 ± 0.43 | 123.28 ± 12.08 |
| $K_1$ (L/mg) | 70.42 ± 12.22 | 17.06 ± 7.33 |
| $Q_2$ (mg/g) | 5.74 ± 0.36 | 135.48 ± 16.89 |
| $K_2$ (L/mg) | 0.27 ± 0.07 | 0.04 ± 0.02 |
| $R^2$ | 0.997 | 0.977 |
| SD(%) | 0.86 | 3.44 |

**Table 3**
Comparison of adsorption capacities of clays and other adsorbents for Cr(VI) and RhB.

| Adsorbents | $Q_m$ (mg/g)* | pH | Reference |
|---|---|---|---|
| *Cr(VI)* | | | |
| Fe–Mt | 13.48 | 4 | This study |
| $Fe/Zr_{4:1}$ pillared montmorillonite | 22.34 | 3 | Zhou et al. (2010) |
| Zr pillared montmorillonite | 19.24 | 3 | Zhou et al. (2010) |
| Montmorillonite support magnetite | 13.88 | 3 | Yuan et al. (2009) |
| Chitosan-montmorillonite | 9.36 | 4.5 | An and Dultz (2008) |
| HDPy-bentonite | 19.24 | 4.5 | Dultz et al. (2012) |
| HDTMA-bentonite | 11.96 | 4.5 | Dultz et al. (2012) |
| BE-bentonite | 15.08 | 4.5 | Dultz et al. (2012) |
| *RhB* | | | |
| Fe–Mt | 258.76 | 4 | This study |
| Acid-treated montmoirllonite | 188.67 | 6.9 | Bhattacharyya et al. (2014) |
| Acid-treated kaolinite | 23.70 | 6.9 | Bhattacharyya et al. (2014) |
| Fe-bentonite | 98.62 | 5.0 | Hou et al. (2011) |
| Sodium montmorillonite | 42.19 | 7 | Selvam et al. (2008) |
| Activated carbon | 478.5 | – | Ding et al. (2014) |

* $Q_m$ is the Langmuir adsorption capacity (mg/g).

### 3.3. Effect of pH

In the present study, simultaneous adsorptions of Cr(VI) and RhB onto Fe–Mt were highly dependent on the pH value of the solution and maximum removals of Cr(VI) and RhB occurred at initial pH ~3.0 for Fe–Mt (Fig. 5). The decrease in the adsorptions of Cr(VI) and RhB below pH 3.0 might be attributed to the dehydroxylation of hydroxyl-iron, since evident release of Fe was observed when pH was below 3.0 (Fig. 6). A similar phenomenon was also observed in previous research works (Zhou et al., 2010; Hou et al., 2011). The adsorption capacity of Fe–Mt toward both Cr(VI) and RhB sharply decreased with increase in pH from 4.0 to 10 (Fig. 5). In the pH range of 1.0–6.0, $HCrO_4^-$ is the predominant species of Cr(VI) while above pH 6.0, Cr (VI) exists mainly as $CrO_4^{2-}$ (Weng et al., 2008). With increase in pH, the observed decrease in Cr(VI) adsorption onto Fe–Mt might be due to the competitive adsorption between $OH^-$ and Cr(VI) anions (Zhou et al., 2010). In addition, according to Zhou et al. (2010), the $pH_{zpc}$ value of Fe–Mt is about 5.8, hence the positive charge on the surface of Fe–Mt decreased with increase in pH, resulting in weaker electrostatic attraction between Fe–Mt and Cr(VI) anions. For the adsorption of RhB, the zwitterionic form of RhB increased when the pH value was above 4.0, which was unfavourable for the adsorption of RhB onto Fe–Mt (Hou et al., 2011). The released amount of Fe dramatically increased when the pH value was below 3.0 (Fig. 6); hence pH range of 3.0–4.0 was the optimum pH value for the simultaneous adsorption of Cr(VI) and RhB onto Fe–Mt.

### 3.4. Adsorption isotherms

Equilibrium adsorption studies were performed to investigate the adsorption capacities and mechanisms of Fe–Mt toward Cr(VI) and RhB. The uptakes of Cr(VI) and RhB on Fe–Mt were quantitatively evaluated using the one or two-site Langmuir model:

$$q_e = \sum_{i=1}^{m} \frac{K_i C_e}{1 + K_i C_e} Q_i \tag{5}$$

where $q_e$ is the adsorption capacity at equilibrium (mg/g), $C_e$ is the equilibrium concentration of Cr(VI) or RhB in the solution (mg/L), $m$ is the number of energetically different adsorption sites, $Q_i$ (mg/g) and $K_i$ are the adsorption capacity and isotherm constant, respectively.

The Freundlich model was also used as:

$$q_e = K_F C_e^{\frac{1}{n}} \tag{6}$$

where $q_e$ and $C_e$ are as described in the Langmuir model, $n$ is constant related to the energy of adsorption and $K_F$ is a physical constants related to adsorption capacity.

The values of normalized standard deviation (SD(%)) were calculated using an equation as:

$$SD(\%) = 100 \times \sqrt{\frac{\sum \left[ \left( q_e^{exp} - q_e^{cal} \right) / q_e^{exp} \right]^2}{N - 1}} \tag{7}$$

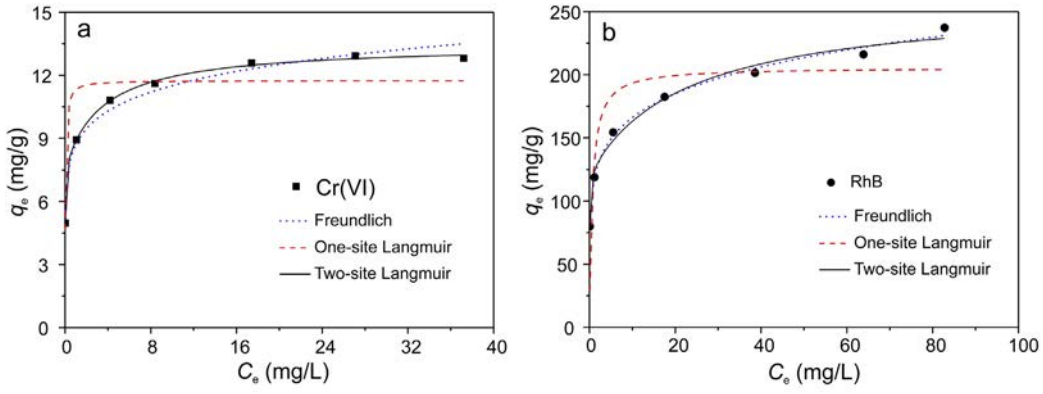


**Fig. 7.** Comparison of the Langmuir and Freundlich isotherms for the simultaneous adsorption of Cr(VI) (a) and RhB (b) on Fe–Mt.

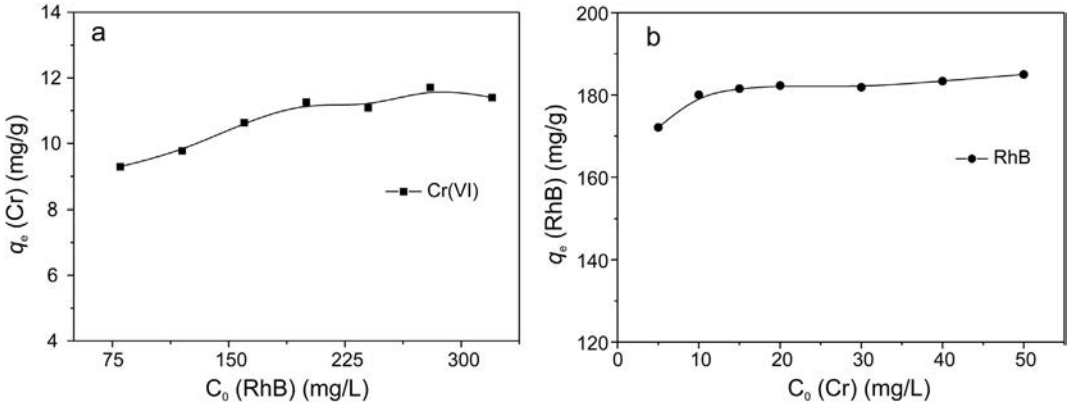


**Fig. 8.** (a) The effect of initial concentration of RhB on the adsorbed amount of Cr(VI) on Fe–Mt ($C_{0,Cr}$ = 15 mg/L); (b) The effect of initial concentration of Cr(VI) on the adsorbed amount of RhB on Fe–Mt ($C_{0,RhB}$ = 200 mg/L).

where the superscripts "exp" and "cal" are the experimental and calculated values with the fitted parameters and *N* is the number of measurements.

The values of the isotherm constants in Table 2 were determined by fitting the above equations to the experimental data. To assess the different isotherms and their validity to correlate experimental results, the experimental data and the theoretical plots for each isotherm could be shown together (Fig. 7). The Freundlich model presented a better fit for Cr(VI) adsorption data than the one-site Langmuir isotherm (Fig. 7a). As indicated by the $R^2$ (Table 2); however, the two-site Langmuir model fitted the experimental results even better, suggesting the existence of heterogeneity (Karamanis and Assimakopoulos, 2007). The SD(%) value and error of estimated parameters were very low, indicating a very good mathematical fit. The two-site Langmuir constants for the adsorption of Cr(VI) showed that the high-affinity sites exist with slight higher adsorption maximum (57%) than that of low-affinity (43%). For the adsorption of RhB, the high SD(%) value at 28.73 of the one-site Langmuir model was dramatically reduced to 3.44 with the application of the two-site Langmuir model (Table 2). The determined constants of two-site Langmuir models showed that high and low affinity sites exist with comparable adsorption capacities at 48% and 52%, respectively. According to the $R^2$ value, Freundlich model described RhB adsorption on Fe–Mt even better (Table 2). The empirical Freundlich model is applicable to multilayer adsorption on heterogeneous surface (Foo and Hameed, 2010). The observed better fit of the experimental data with Freundlich isotherm can be attributed to heterogeneous distribution of active sites on Fe–Mt (Karamanis and Assimakopoulos, 2007; Foo and Hameed, 2010). The Freundlich coefficients, $1/n$, are <1, indicating that the adsorptions of Cr(VI) and RhB on Fe–Mt are favourable.

Although some other clay-based materials had been used to removal Cr(VI) or RhB from water (Table 3), simultaneous adsorption behaviours of Cr(VI) and RhB on clay minerals were seldom reported. Compared to these reported absorbents, Fe–Mt as a low-cost and rapid adsorbent shows comparable adsorption capacities toward both Cr (VI) and RhB, which is desirable for the treatment and purification of wastewater samples and soils containing both pollutants.

**Table 4**
Desorption of adsorbed Cr(VI) and RhB by repeated equilibration with 0.01 M KCl in the simultaneous system.

| Adsorbates | Amount adsorbed (mg/g) | Amount desorbed (mg/g) | | | | % Desorbed |
|---|---|---|---|---|---|---|
| | | 1st | 2nd | 3rd | Total | |
| Cr(VI) | 10.78 | 1.03 | 0.37 | 0.21 | 1.61 | 14.9 |
| RhB | 181.99 | 11.08 | 5.20 | 1.66 | 17.94 | 9.9 |

### 3.5. Effect of the coexist contaminant

To better understand the simultaneous adsorption behaviours of Cr (VI) and RhB on Fe–Mt, the effects of initial concentration of one contaminant on the adsorption of the other one were investigated (Fig. 8). The adsorbed amount of Cr(VI) on Fe–Mt increased with increase in initial concentration of RhB (Fig. 8a). When the initial concentration of RhB exceeded 200 mg/L, the adsorption gradually reached its maximum. With increase in initial concentration of Cr(VI), the adsorption of RhB on Fe–Mt was also enhanced (Fig 8b), which reached its maximum when the initial concentration of Cr(VI) was higher than 10 mg/L. These findings suggest that the adsorption of Cr(VI) and RhB on Fe–Mt is without competition and the adsorbed contaminant may provide additional sites for the adsorption of the other contaminant.

In previous studies, the possible mechanisms for the synergistic adsorption of heavy metal cations and oxyanions on metal (oxyhydro) oxide include the formation of ternary complexes, surface precipitation, and enhanced electrostatic interaction (Collins et al., 1999; Grafe et al., 2004; Swedlund et al., 2009; Elzinga and Kretzschmar, 2013; Zhu et al., 2014; Ma et al., 2015). Zhu et al. (2014) have reported that the synergistic adsorption of Cd(II) and phosphate on hydroxyiron-montmorillonite complexes could be attributed to the formation of P-bridge ternary complexes on the adsorbent surface. However, the properties of RhB are very different from that of heavy metal cations. Therefore the possible mechanism of synergistic adsorption of Cr(VI) and RhB need to be further studied using spectroscopic methods and mechanical calculations.

### 3.6. Desorption processes

Besides for a better understand the adsorption process, desorption experiments also give insight into the long-term stability of the adsorbed contaminants, which is of great importance in wastewater treatment application. With three consecutive steps of equilibration with 0.01 M KCl, 14.9% of Cr(VI) and 9.9% of RhB were totally released from saturated Fe–Mt, and most of released Cr(VI) and RhB were remobilized to the solution phase during the first desorption cycle (Table 4). The low desorption amounts of Cr(VI) and RhB suggest the high affinity of two contaminants for Fe–Mt.

## 4. Conclusion

The results of this study indicate that the hydroxyiron-montmorillonite is a very promising adsorbent for the removal of hexavalent chromium (Cr(VI)) and rhodamine B (RhB) from aqueous solution simultaneously. The adsorptions of Cr(VI) and RhB on Fe–Mt follow the pseudo-second order model. The adsorption rates and

capacities of Fe–Mt toward Cr(VI) and RhB were slightly higher than those in the corresponding single adsorption systems. The most effective pH range was found to be 3.0–4.0 for the removal of both contaminants. The adsorption isotherm of Cr(VI) was best fitted with the two-site Langmuir model while RhB isotherm best followed the Freundlich model. For both contaminants, the adsorption of one contaminant increased with increase in the initial concentration of the other one. Therefore, Cr(VI) and RhB could be simultaneously adsorbed onto Fe–Mt and this offers a potentially useful method for the simultaneous removal of these pollutants from the environment.

## Acknowledgements

This research was supported by the Queensland University of Technology's Vice Chancellor's research grant. Dr. Xi is grateful to the financial support from the CAS-SAFEA International Partnership Programme for Creative Research Team (Grant No. 20140491534). We thank Tony Raftery and Mitchell De Bruyn from Central Analytical Research Facility (CARF, IFE) of Queensland University of Technology for assistance with the XRD and ICP-OES analyses, respectively. The first author also thanks the Youth Innovation Promotion Association CAS (Grant No. 2014324) and China Scholarship Council (CSC) for financial support.

## References

An, J.-H., Dultz, S., 2008. Adsorption of Cr (VI) and As (V) on chitosan-montmorillonite: selectivity and pH dependence. Clay Clay Miner. 56, 549–557.
Bergaya, F., Lagaly, G., 2013. Chapter 1 — general introduction: clays, clay minerals, and clay science. In: Bergaya, F., Lagaly, G. (Eds.), Developments in Clay Science Vol. 5A. Elsevier, pp. 1–19.
Bhattacharyya, K.G., SenGupta, S., Sarma, G.K., 2014. Interactions of the dye, Rhodamine B with kaolinite and montmorillonite in water. Appl. Clay Sci. 99, 7–17.
Borgnino, L., Giacomelli, C.E., Avena, M.J., De Pauli, C.P., 2010. Phosphate adsorbed on Fe (III) modified montmorillonite: surface complexation studied by ATR-FTIR spectroscopy. Colloid Surface A 353, 238–244.
Collins, C.R., Ragnarsdottir, K.V., Sherman, D.M., 1999. Effect of inorganic and organic ligands on the mechanism of cadmium sorption to goethite. Geochim. Cosmochim. Acta 63, 2989–3002.
Ding, L., Zou, B., Gao, W., Liu, Q., Wang, Z., Guo, Y., Wang, X., Liu, Y., 2014. Adsorption of Rhodamine-B from aqueous solution using treated rice husk-based activated carbon. Colloids and Surfaces A 446, 1–7.
Dultz, S., An, J.H., Riebe, B., 2012. Organic cation exchanged montmorillonite and vermiculite as adsorbents for Cr(VI): effect of layer charge on adsorption properties. Appl. Clay Sci. 67-68, 125–133.
Elzinga, E.J., Kretzschmar, R., 2013. In situ ATR-FTIR spectroscopic analysis of the co-adsorption of orthophosphate and Cd(II) onto hematite. Geochim. Cosmochim. Acta 117, 53–64.
Fisher, P., 1999. Review of using Rhodamine B as a marker for wildlife studies. Wildl. Soc. Bull. 318-329.
Foo, K.Y., Hameed, B.H., 2010. Insights into the modeling of adsorption isotherm systems. Chem. Eng. J. 156, 2–10.
Grafe, M., Nachtegaal, M., Sparks, D.L., 2004. Formation of metal-arsenate precipitates at the goethite–water interface. Environ Sci Technol 38, 6561–6570.
Ho, Y.S., McKay, G., 1999. Pseudo-second order model for sorption processes. Process Biochem. 34, 451–465.
Hou, M.F., Ma, C.X., Zhang, W.D., Tang, X.Y., Fan, Y.N., Wan, H.F., 2011. Removal of rhodamine B using iron-pillared bentonite. J. Hazard. Mater. 186, 1118–1123.
Karamanis, D., Assimakopoulos, P.A., 2007. Efficiency of aluminum-pillared montmorillonite on the removal of cesium and copper from aqueous solutions. Water Res. 41, 1897–1906.
Ma, L., Zhu, J., Xi, Y., Zhu, R., He, H., Liang, X., Ayoko, G.A., 2015. Simultaneous adsorption of Cd(II) and phosphate on $Al_{13}$ pillared montmorillonite. RSC Adv 5, 77227–77234.
Matthes, W., Madsen, F.T., Kahr, G., 1999. Sorption of heavy-metal cations by Al and Zr-hydroxy-intercalated and pillared bentonite. Clay Clay Miner. 47, 617–629.
Salgado-Gómez, N., Macedo-Miranda, M.G., Olguín, M.T., 2014. Chromium VI adsorption from sodium chromate and potassium dichromate aqueous systems by hexadecyltrimethylammonium-modified zeolite-rich tuff. Appl. Clay Sci. 95, 197–204.
Schlegel, M.L., Manceau, A., 2007. Zn incorporation in hydroxy-Al- and Keggin $Al_{13}$-intercalated montmorillonite: a powder and polarized EXAFS study. Environ Sci Technol 41, 1942–1948.
Selvam, P.P., Preethi, S., Basakaralingam, P., Thinakaran, N., Sivasamy, A., Sivanesan, S., 2008. Removal of rhodamine B from aqueous solution by adsorption onto sodium montmorillonite. J. Hazard. Mater. 155, 39–44.
Sparks, D.L., 2005. Toxic metals in the environment: the role of surfaces. Elements 1, 193–197.
Swedlund, P.J., Webster, J.G., Miskelly, G.M., 2009. Goethite adsorption of Cu(II), Pb(II), Cd (II), and Zn(II) in the presence of sulfate: properties of the ternary complex. Geochim. Cosmochim. Acta 73, 1548–1562.
Undabeytia, T., Nir, S., Rytwo, G., Morillo, E., Maqueda, C., 1998. Modeling adsorption-desorption processes of Cd on montmorillonite. Clay Clay Miner. 46, 423–428.
USEPA, 2014. TSCA work plan for chemical assessments: 2014 update, in: Agency, U.S. Envrionmental Protection Agency (Ed.).
Weng, C.-H., Sharma, Y.C., Chu, S.-H., 2008. Adsorption of Cr(VI) from aqueous solutions by spent activated clay. J. Hazard. Mater. 155, 65–75.
Wu, P.X., Wu, W.M., Li, S.Z., Xing, N., Zhu, N.W., Li, P., Wu, J.H., Yang, C., Dang, Z., 2009. Removal of $Cd^{2+}$ from aqueous solution by adsorption using Fe–montmorillonite. J. Hazard. Mater. 169, 824–830.
Yan, L.G., Shan, X.Q., Wen, B., Owens, G., 2008. Adsorption of cadmium onto $Al_{13}$-pillared acid-activated montmorillonite. J. Hazard. Mater. 156, 499–508.
Yan, L.G., Xu, Y.Y., Yu, H.Q., Xin, X.D., Wei, Q., Du, B., 2010. Adsorption of phosphate from aqueous solution by hydroxy-aluminum, hydroxy-iron and hydroxy-iron-aluminum pillared bentonites. J. Hazard. Mater. 179, 244–250.
Yuan, G.D., Theng, B.K.G., Churchman, G.J., Gates, W.P., 2013. Chapter 5.1 — clays and clay minerals for pollution control. In: Bergaya, F., Lagaly, G. (Eds.), Developments in Clay Science Vol. 5B. Elsevier, pp. 587–644.
Yuan, P., Annabi-Bergaya, F., Tao, Q., Fan, M.D., Liu, Z.W., Zhu, J.X., He, H.P., Chen, T.H., 2008. A combined study by XRD, MR, TG and HRTEM on the structure of delaminated Fe-intercalated/pillared clay. J. Colloid Interface Sci. 324, 142–149.
Yuan, P., Fan, M.D., Yang, D., He, H.P., Liu, D., Yuan, A.H., Zhu, J.X., Chen, T.H., 2009. Montmorillonite-supported magnetite nanoparticles for the removal of hexavalent chromium [Cr(VI)] from aqueous solutions. J. Hazard. Mater. 166, 821–829.
Yuan, P., Liu, D., Fan, M.D., Yang, D., Zhu, R.L., Ge, F., Zhu, J.X., He, H.P., 2010. Removal of hexavalent chromium [Cr(VI)] from aqueous solutions by the diatomite-supported/unsupported magnetite nanoparticles. J. Hazard. Mater. 173, 614–621.
Zhou, J.B., Wu, P.X., Dang, Z., Zhu, N.W., Li, P., Wu, J.H., Wang, X.D., 2010. Polymeric Fe/Zr pillared montmorillonite for the removal of Cr(VI) from aqueous solutions. Chem. Eng. J. 162, 1035–1044.
Zhu, L.Z., Zhu, R.L., 2007. Simultaneous sorption of organic compounds and phosphate to inorganic–organic bentonites from water. Sep. Purif. Technol. 54, 71–76.
Zhu, M.X., Ding, K.Y., Xu, S.H., Jiang, X., 2009. Adsorption of phosphate on hydroxyaluminum- and hydroxyiron-montmorillonite complexes. J. Hazard. Mater. 165, 645–651.
Zhu, R.L., Li, M., Ge, F., Xu, Y., Zhu, J.X., He, H.P., 2014. Co-sorption of cd and phosphate on the surface of a synthetic hydroxyiron-montmorillonite complex. Clay Clay Miner. 62, 79–88.